Urol Res (1999) 27:426–431

ORIGINAL PAPER

Y. Shirane · Y. Kurokawa · S. Miyashita
H. Komatsu · S. Kagawa

Study of inhibition mechanisms of glycosaminoglycans on calcium oxalate monohydrate crystals by atomic force microscopy

Received: 23 November 1998 / Accepted: 25 June 1999

Abstract Atomic force microscopy (AFM) was applied to the (-101) faces of calcium oxalate monohydrate (COM) crystals grown from calcium oxalate (CaOx) solutions. Microstructures of many spiral hillocks with step height of 1 nm were observed on the faces. Then using AFM in situ, we analysed the re-growth process of the spiral steps on the face of COM seed-crystals in CaOx growth solutions that contained growth inhibitors of glycosaminoglycans and studied their inhibition mechanisms on COM crystals. The total morphology of the faces of COM seed crystals re-grown in the CaOx growth solutions was assessed by scanning electron microscopy (SEM). In the growth solution without glycosaminoglycans (control experiment) or with chondroitin sulphate (ChS), AFM images and SEM micrographs of the faces of the re-grown seed crystals showed two-dimensional (2D) nucleation although 2D nucleation was delayed in the presence of ChS. However, the addition of dermatan sulphate (DS) to the growth solution resulted in isotropic growth by a step flow mode and spiral mechanism. With regard to the main inhibition mechanisms of two glycosaminoglycans (ChS and DS) on COM crystals, it can be concluded from these results that ChS delays 2D nucleation and DS inhibits 2D nucleation.

Key words Calcium oxalate monohydrate · Glycosaminoglycans · Atomic force microscopy · Inhibition mechanisms · Two-dimensional nucleation · Spiral growth

Y. Shirane (✉) · Y. Kurokawa · S. Kagawa
Department of Urology, The University of Tokushima, School of Medicine, Tokushima 770–8503, Japan
e-mail: shirane@clin.med.tokushima-u.ac.jp
Tel.: +81-88-633-7159; Fax: +81-88-633-7160

S. Miyashita · H. Komatsu
Tohoku University, Institute for Materials Research, Sendai 980–8577, Japan

Introduction

Calcium oxalate monohydrate (COM) is a major inorganic component of kidney stones. There are many papers about inhibitors of COM crystallization, including nucleation, growth and aggregation processes. Glycosaminoglycans (GAGs) are well-known macromolecular inhibitors found in urine and kidney stones. In general, growth inhibitors of COM crystals have been thought to exert their effects at certain sites on the crystal surface, so-called growth sites [3, 5, 10] or binding sites [4, 9]. Our previous morphological studies on COM also suggest that GAGs bind to the crystal surfaces in a regular fashion rather than at random, depending on their species [7, 8]. The binding sites seem to be calcium sites on the faces matching negatively charged side groups on the GAG chains. However, no one has yet shown the exact binding sites as well as the detailed microstructures of the COM crystal faces. One of the reasons for this is the lack of appropriate techniques to observe the crystal surfaces without causing topographic damage. Although scanning electron microscopy (SEM) has been extensively used to investigate the surface morphology of a variety of samples, these samples require special treatments, such as drying in vacuum and coating, that lead to surface denaturalization. Moreover, SEM induces topographic damage caused by the electron beam acting on heat-unstable COM, as shown in the thermal analysis data, and also does not give direct real vertical (Z) information. A recently developed technique, atomic force microscopy (AFM) not only has a high resolution, but also can observe samples without precoating and monitor their real time growth processes in solution. AFM thus has been used to investigate the surface topography of various kinds of crystals and biological specimens, including urinary oxalate stones [2], cells, and proteins, for example. In the present study, we report the surface morphology of uncoated COM crystals observed by AFM in two different environments: first, by observing the (-101) faces of COM crystals in air; and second, by observing

the re-growth process of the faces of COM seed-crystals in calcium oxalate (CaOx) growth solutions in the presence or absence of inhibitors. In addition, we also show scanning electron micrographs of the faces of COM seed-crystals re-grown in the growth solutions with or without inhibitors to complement the AFM. Finally, we discuss the inhibition mechanisms of GAGs on COM crystals.

Material and methods

Solution preparation

Chondroitin 6-suphfate (ChS) and dermatan sulphate (DS) were purchased from Seikagaku Kogyo (Tokyo, Japan) and all other reagent-grade chemicals from Wako Pure Chemicals (Osaka, Japan). Milli-Q water (Millipore Systems, Bedford, USA) was used for preparation of all solutions. Stock solutions of 10 mM calcium chloride, 1 mM sodium oxalate and 1 mg/ml GAGs were prepared using 50 mM sodium acetate buffer (pH 5.7) containing 100 mM sodium chloride and were filtered through a 0.22 μm Millipore filter. The CaOx solutions for COM crystal preparation initially contained 4 mM calcium chloride and 0.2 mM sodium oxalate in the acetate buffer. Either low or high supersaturated CaOx growth solutions for re-growth of COM seed-crystals were prepared. These were composed of the same concentration of calcium, 4 mM and differing concentrations of oxalate, 0.0625 or 0.1 mM, with GAG, 30 μg/ml in acetate buffer. The growth solutions in control experiments did not contain any GAGs.

Crystal preparation

The COM crystals were prepared under conditions close to physiological ones, such as the temperature (37°C), the ionic strength (150 mM) and the pH (5.7). The initial concentrations of calcium (4 mM) and oxalate (0.2 mM) were also used within their normal urinary ranges. Appropriate amounts of calcium chloride stock solution and acetate buffer were measured into plastic wells containing a few small glass-plates (less than 1 cm^2) or round cover-glasses (15 mm in diameter) and were preincubated for 30 min. Then, sodium oxalate stock solution, which was also preincubated, was added dropwise to the above solutions in each well to initiate crystal formation. The wells were kept in an incubator for 7 days to allow the crystals to mature. The glass plate or cover-glass substrates on which the crystals formed were then picked up, rinsed with distilled water several times and air-dried at room temperature. The crystals on the small glass plate substrates were used for AFM observation in air. The crystals on the round cover-glass substrates were used as seed crystals for the following in situ AFM or SEM observation. The COM crystals grown under these conditions had elongated hexagonal (-101) faces that were well developed and thus were easy to observe (Fig. 1). The faces of COM crystals were indexed after the unit cell reported by Deganello and Piro [1].

Observation by AFM

Direct observations in air of the crystals on glass plate substrates were carried out using a NanoScope II atomic force microscope (Digital Instruments, Santa Barbara, USA). All AFM images presented in this study were taken in the constant "height mode". In the case of in situ observation of the re-growth process, a cover-glass substrate with seed crystals was transferred into a sealed growth cell attached to the atomic force microscope. Appropriate spiral steps on the (-101) face of a seed-crystal were initially chosen for observation, and then the growth cell was filled with the growth solution using a syringe. The entire system was kept in a thermostated room at 20°C, and AFM images of the re-growth process of the spiral steps were obtained in real time.

Observation by SEM

To confirm the total morphology of the faces re-grown in the AFM growth cell during in situ observation, seed-crystals on the other cover-glass substrates were re-grown for 5 h in the growth solution at a high supersaturation with or without GAGs at 20°C, the same temperature used for in situ AFM. The cover-glass substrates with the seed crystals were then rinsed with distilled water, air-dried, coated with gold/palladium (10 nm thick) and subjected to a HITACHI S-800 scanning electron microscope (HITACHI, Tokyo, Japan) operated at 10 kV.

Results

AFM observation of the (-101) faces of COM crystals in air

The AFM image of the (-101) face of COM crystals grown from the CaOx solutions revealed many spiral hillocks on the wide terraces of the face. The hillocks had slopes composed of many wavy-edged steps which were approximately 1 nm in height (Fig. 2). This Z

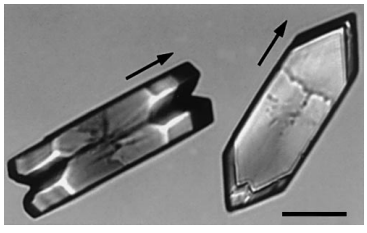

Fig. 1 Differential interference micrograph of typical shape of COM crystals grown in CaOx solutions without GAGs. *Right*, (-101) face view of crystal with the hexagonal face elongated along [101] direction. *Left*, (010) face view of other crystal. *Black arrows* indicate [101] direction. *Bar* = 10 μm

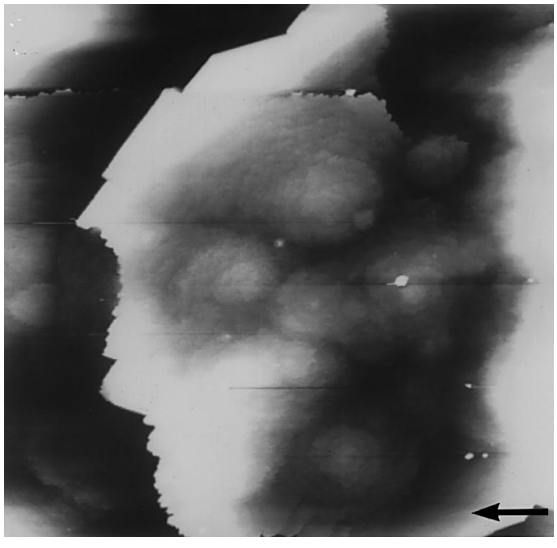

Fig. 2 AFM image, obtained in air, of the (-101) face of COM crystal grown in CaOx solutions without GAGs shows many spiral hillocks on the wide terraces of the face. *Black arrow* indicates [101] direction. *Image size*, 10 μm × 10 μm

information was obtained directly from the image. However, these surface microstructures have never been observed by SEM.

In situ AFM observation of the (-101) faces of COM seed-crystals

Figure 3 shows in situ AFM images of the control experiments. The images taken under the growth solution at low supersaturation showed that the step edges of the spiral hillocks were clear 20 min after the introduction of the solution (Fig. 3A). The image became spotty and obscure 40 min later due to the formation of two-dimensional (2D) nuclei or islands on the terraces and step edges (Fig. 3B), and then was further disturbed by signal noise 60 min later (Fig. 3C). The images taken for the growth solution at high supersaturation were obscure and disturbed by signal noise from the early stages (at 15 min) of re-growth (data not shown).

When the growth solution at low supersaturation contained ChS, the step edges of spiral hillocks in the AFM image did not change over the first hour, but after 3 h they became obscure to the same extent as those in the control image (data not shown).

In contrast, the AFM images of the crystals re-grown in the growth solution at high supersaturation containing DS (Fig. 4) were still clear and showed dynamic growth morphologies even 5 h after starting the re-growth. The smooth step edges of spiral hillocks at the early stages (Fig. 4A) roughened 3 h later (Fig. 4B) and then became thick and sharply serrated in the [101] direction 5 h later (Fig. 4C). The steps advanced in all directions. However, dynamic growth kinetics could not be measured due to a difficulty in finding a fixed point suitable to use as a landmark for calculating growth rates of the steps in the images.

SEM observation of the (-101) face of re-grown COM seed-crystals

The (-101) face of the non-treated seed crystal in the scanning electron micrograph exhibited faint layers (Fig. 5A). The face of the seed-crystals re-grown in the control experiment revealed many newly grown parts that were very thick and non-uniformly distributed (Fig. 5B). The layer-edges in the [101] direction were sharply serrated with {011} facets. The face of the seed crystals re-grown in the presence of ChS also showed newly grown parts that extended regularly along the layer edges (Fig. 5C) and were thinner than those shown in the control micrograph (Fig. 5B). The layer edges in the [101] direction were also serrated with {011} facets. On the other hand, a composite spiral pattern was clearly seen on the face of the seed crystals re-grown in

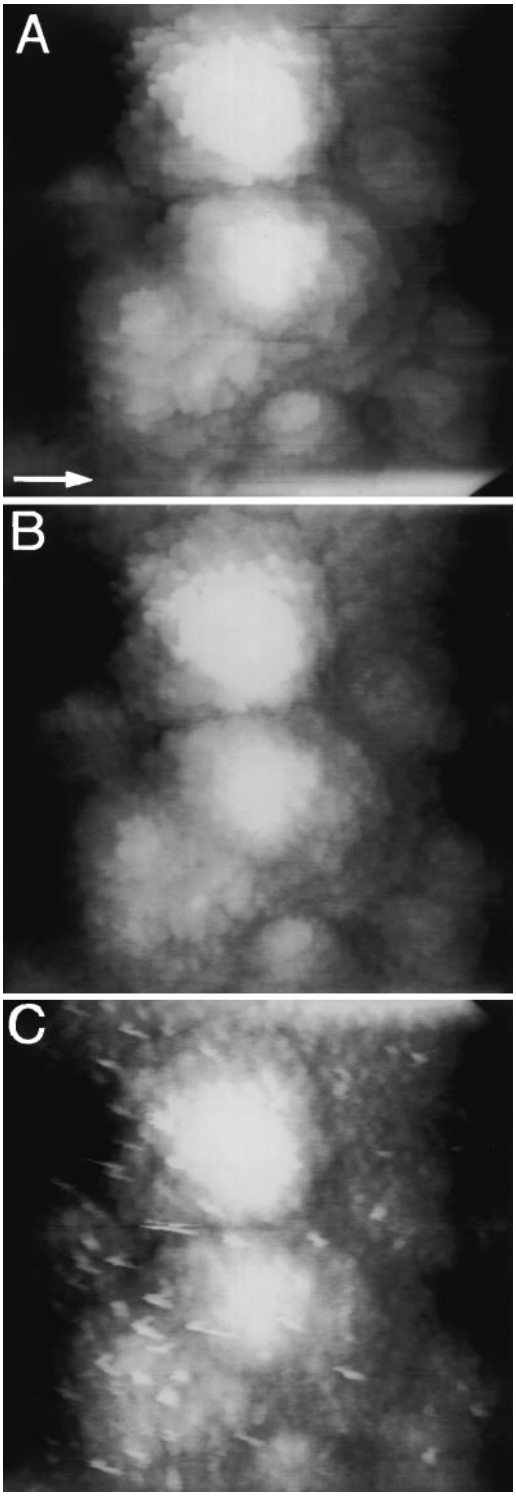

Fig. 3A–C In situ AFM images of the spiral steps on the (-101) face of COM seed-crystal grown for 20 min (**A**), 40 min (**B**) and 60 min (**C**) in CaOx growth solution at low supersaturation without GAGs. The spotty and obscure image (**B**) is due to the formation of 2-D nuclei or islands on the terraces and step-edges, and the disturbed image (**C**) is caused by signal noise. *White arrow* indicates [101] direction. *Image size*, 4 μm × 4 μm

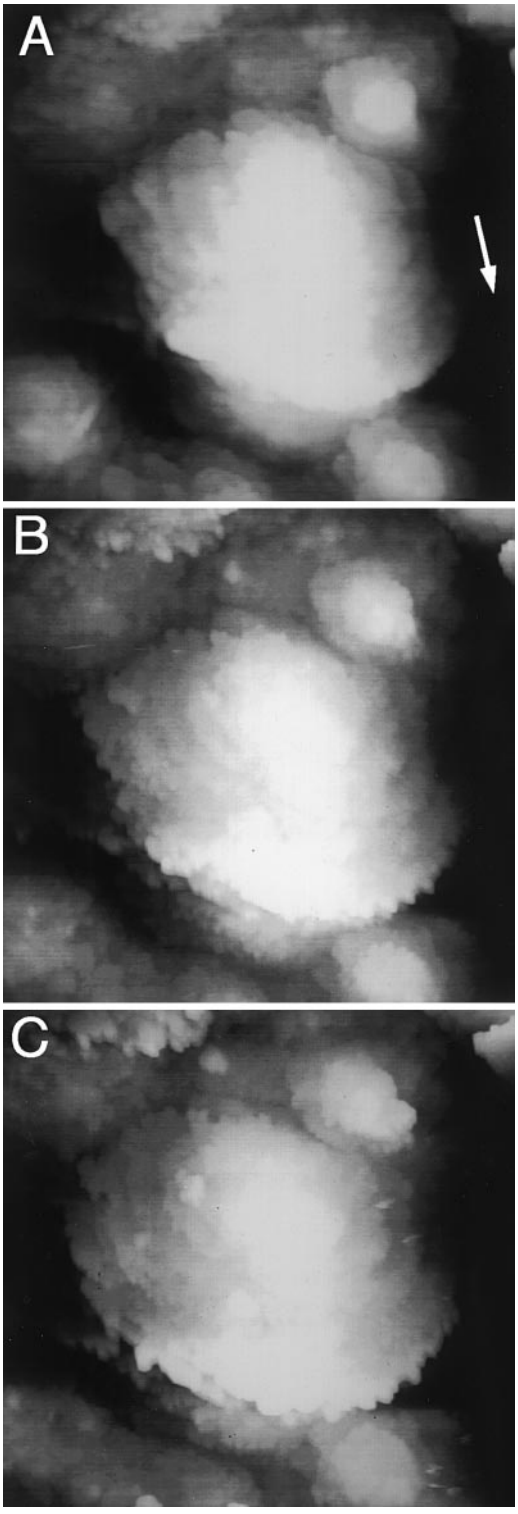

Fig. 4A–C In situ AFM images of the spiral steps on the (-101) face of COM seed crystal grown for 10 min (**A**), 3 h (**B**) and 5 h (**C**) in CaOx growth solution at high supersaturation with DS. The clear images show the roughened (**B**) and thick (**C**) step edges sharply serrated in the [101] direction. The steps advance isotropically. *White arrow* indicates [101] direction. *Image size*, 5 μm × 5 μm

the presence of DS (Fig. 5D). The layer edges were round in the [101] direction and had no {011} facets in the central area. The layers in the spiral pattern were higher than those of the non-treated seed-crystals (Fig. 5A), but it was impossible to measure their height from the scanning electron micrographs.

Discussion

In this paper we have shown, for the first time, AFM images of the (-101) faces of COM crystals and in situ AFM images of the spiral steps in growth solutions with or without GAGs, and we have discussed the inhibition mechanisms of GAGs on COM crystals. While SEM is an established technique for surface observations and can clearly show the features of the surfaces, it has never revealed fine surface microstructures such as the spiral hillocks in the AFM images. In the case of SEM, samples are coated with metals of 10 nm in thickness that might mask some structures, and the SEM is less sensitive to height differences (Z information) [6]. In contrast, AFM can image the COM surfaces in their native uncoated states without causing topographic damage and can provide Z information directly. In spite of such excellent features, AFM in air has one problem: it is unable to scan crystals with optically rough surfaces, such as COM crystals consisting of many layers of lamellae generated from CaOx solutions in the presence of some GAG species (heparin, heparan sulphate and DS) [7, 8]. In such a case, this difficulty can be overcome by in situ AFM of seed crystals in solution that have spiral steps on the (-101) faces; that is, by observing the re-growth process of the spiral steps in a solution containing those GAGs. This provides a great advantage in clarifying the growth inhibition mechanisms of GAGs on COM crystals. In this experiment, the growth kinetics of the steps could not be analysed because a fixed point was not available in the images. An improved AFM technique would give us the exact step growth rate and detail at the molecular level of binding sites as well as the morphologies.

When the growth solution contains neither ChS nor DS, 2D nucleation occurs freely on the faces and results in spotty and obscure AFM images (Fig. 3). Quick 2D nucleation growth is also indicated by the very thick and irregularly distributed re-grown parts in a scanning electron micrograph (Fig. 5B). Therefore, 2D nucleation is the dominant growth mode of the COM seed crystals at early stages of re-growth since the supersaturation is still high. However, the spiral hillocks on the seed crystals (Fig. 2) suggest spiral growth mode prevails under low saturated conditions at the final stages of seed crystal preparation. These observations are not contradictory, but rather represent early and later stages

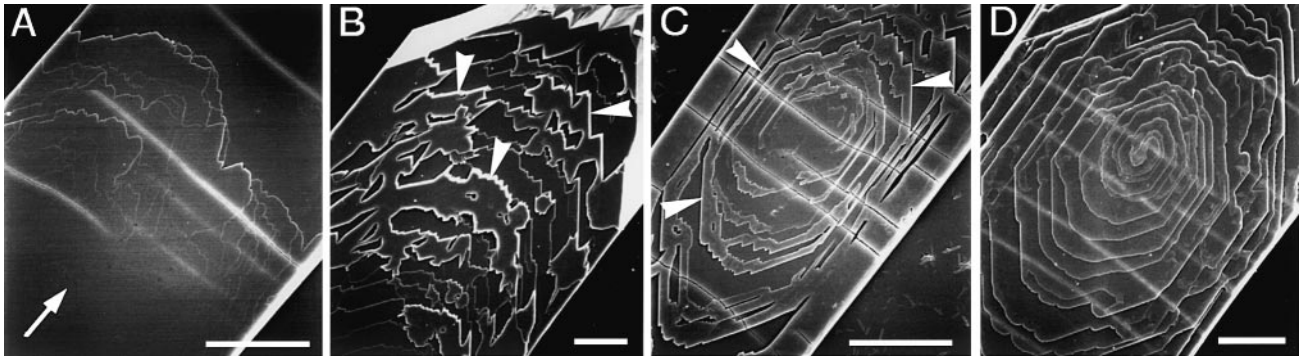

Fig. 5A–D Scanning electron micrographs of the (-101) faces of non-treated seed crystal (**A**) and of seed crystals re-grown for 5 h in the growth solution at high supersaturation without GAGs (**B**), or with ChS (**C**), or DS (**D**). The very thick newly grown parts (*white arrowheads*), indicating 2D nucleation growth, are irregularly distributed on the face. The layer-edges are serrated in the [101] direction (**B**). The newly grown parts (*white arrowheads*) are located along the layer-edges, which are serrated in the [101] direction (**C**). Composite spiral pattern, indicating spiral growth, with the rounded layer-edges in the [101] direction (**D**). *White diagonal lines* in the images are surface cracks damaged by electron beam. *White arrow* indicates [101] direction. *Bar* = 10 μm in all

occurring as the concentration of the solutes decreases as the crystals grow.

The addition of ChS to the growth solution causes a time lag in the appearance of 2D nuclei or islands and a consequent time lag in the development of the obscure AFM images. The scanning electron micrograph of the re-grown face shows 2D nucleation growth along the layer edges (Fig. 5C). These results indicate that ChS delays 2D nucleation and regulates the growth direction and the settling location site of the 2D nuclei, resulting in the neat crystal morphology as mentioned in the previous paper [7].

The AFM image of the face re-grown with DS for 5 h is still clear and shows the steps advancing isotropically (Fig. 4), indicating that DS inhibits 2D nucleation, induces step flow growth and deprives the anisotropic nature of COM growth. The resulting face in the SEM exhibits a composite spiral pattern (Fig. 5D). Thus, DS seems to change the growth mode from 2D nucleation to a spiral mechanism so that there is a change from high driving force conditions to lower ones. Because the concentrations of DS used here were too low to directly decrease the Ca^{2+} concentration, it is thought that DS might act through unknown mechanisms after binding to the crystals, possibly diminishing the chemical potential of the solution around the crystals rather than that of the bulk solution and thus inhibiting the development of 2D nuclei. DS could inhibit the quick 2D growth of COM crystals in urine that contains high concentrations of calcium and/or oxalate, as occurs after a meal. The sharply serrated step edges in the [101] direction in the microview of AFM images (Fig. 4B, C) seem to conflict with the smooth and round layer-edges in the [101] direction in the macroview of a SEM (Fig. 5D). It may be explained by DS sporadically binding to the steps advancing in the [101] direction with the result that the growth anisotropy of the steps is lost in spite of the dominant growth in the [101] direction in the absence of DS. Consequently, no facet forms and the round layer-edges develop.

Our previous results show that ChS and DS differ in their effects on the morphology of COM crystals. Furthermore, only DS is contained in the crystals grown in solutions with the same concentrations of either ChS or DS [7, 8]. DS seems to have a strong interaction with the crystal surfaces and to be present in the crystals, while ChS seems to have weak interaction with the surfaces, resulting in no inclusion. The results of this study provide additional evidence for the differing inhibitory mechanisms of ChS and DS on COM crystals. It is likely that these differences in the effects of the two GAGs on COM crystals are caused by their stereo structure that might lead to the different binding manner and binding sites on the crystals. Among GAGs, both ChS and DS have similar repeating disaccharide sequences, as reflected in the fact that DS has been referred to as chondroitin sulphate B. However, their uronic acid moieties are stereo isomers which could cause large differences in their molecular conformation.

Further studies and refinements in the AFM technique may allow us to elucidate the cause of these differences in the inhibitory mechanisms of GAGs on COM crystals.

Acknowledgement The authors have benefited from the inter-university cooperative research program of the Institute for Materials Research in Tohoku University.

References

1. Deganello S, Piro OE (1981) The crystal structure of calcium oxalate monohydrate (whewellite). Neues Jahrb Mineral Monatsh 2:81
2. Dorian HH, Rez P, Drach GW (1996) Evidence for aggregation in oxalate stone formation: atomic force and low voltage scanning electron microscopy. J Urol 156:1833
3. Fellström B, Lindsjö M, Danielson BG, Karlsson FA, Ljunghall S (1989) Binding of glycosaminoglycan inhibitors to calcium oxalate crystals in relation to ionic strength. Clin Chim Acta 180:213
4. Fleish H (1978) Inhibitors and promoters of stone formation. Kidney Int 13:361
5. Kok DJ, Papapoulos SE, Blomen LJMJ, Bijvoet OLM (1988) Modulation of calcium oxalate monohydrate crystallization kinetics in vitro. Kidney Int 34:346

6. Komatsu H (1985) Optical characterization of crystal surfaces. In: Kaldis E (ed) Crystal growth of electronic materials, 1st edn. North-Holland, Amsterdam, p 359
7. Shirane Y, Kurokawa Y, Sumiyoshi Y, Kagawa S (1995) Morphological effects of glycosaminoglycans on calcium oxalate monohydrate crystals. Scanning Microsc 9:1081
8. Shirane Y, Yamamoto A, Kagawa S (1994) The effect of glycosaminoglycans on calcium oxalate monohydrate crystal morphology. In: Ryall RL, Bais R, Marshall VR, Rofe AM, Smith LH, Walker VR (eds) Urolithiasis 2. Plenum, New York, p 189
9. Shirane Y, Kagawa S (1993) Scanning electron microscopic study of the effect of citrate and pyrophosphate on the calcium oxalate crystal morphology. J Urol 150:1980
10. Worcester EM, Nakagawa Y, Wabner CL, Kumar S, Coe FL (1988) Crystal adsorption and growth slowing by nephrocalcin, albumin, and Tamm-Horsfall protein. Am J Physiol 255:F1197